Original scientific paper

UDK 537.6/.8:621.313/.314
DOI 10.7251/COMEN2302126D

TRANSPORT CHARACTERISTICS OF ELECTRONS IN NITROUS OXIDE (N_2O) UNDER THE INFLUENCE OF CROSSED ELECTRIC AND MAGNETIC DC FIELDS

Snježana Dupljanin[1*], Olivera Šašić[2], Zoran Lj. Petrović[3,4], Dragoljub Mirjanić[5]

[1] Faculty of Science and Mathematics, University of Banja Luka, Banja Luka, Republic of Srpska, Bosnia and Herzegovina
[2] Faculty of Traffic, University of Belgrade, Belgrade, Serbia
[3] Serbian Academy of Sciences and Arts, Belgrade, Serbia
[4] University of Ulster, Jordanstown, Belfast, Northern Ireland, UK
[5] Academy of Sciences and Arts of the Republic of Srpska, Banja Luka, Republic of Srpska, Bosnia and Herzegovina

[*] Corresponding author: snjezana.dupljanin@pmf.unibl.org

Abstract: Monte Carlo (MC) calculations of transport and rate coefficients of an electron swarm moving in nitrous oxide (N_2O) under the influence of DC crossed electric and magnetic orthogonal fields are presented. The set of cross sections for e^-/N_2O scattering obtained in our previous investigations was used as the initial parameter. Calculations of mean energy, drift velocity, diffusion coefficients and rate coefficients for elastic and individual inelastic processes were performed for five different values of the reduced magnetic field (B/N = 100 Hx, 200 Hx, 500 Hx, 1000 Hx and 2000 Hx, 1Hx = 10^{-27} Tm^3), where for each of these values, the value of the reduced electric field (E/N) ranged from 50 Td to 2000 Td (1Td = $10^{-21}Vm^2$). The ratio of cyclotron to total collision frequency in these cases is less than one for all values of B/N (except for the highest one when it is slightly greater than one), so we may claim that our swarm is in a collision-dominated regime. The cooling effect of the swarm is observable, i.e. there is a decrease in its mean energy as the magnetic field increases, as well as a decrease in the drift velocity component in the electric field direction. Electron diffusion is slightly anisotropic for the higher values of B/N.

Keywords: electron swarm, transport coefficients, nitrous oxide.

1. INTRODUCTION

Nitrous oxide (N_2O) is widely used in chemistry, medicine (as an anesthetic) and technology, primarily for doping nitrogen atoms (N) into oxide materials [1] and depositing diamond-like carbon films [2]. In both cases, N_2O is used as an RF plasma background gas for the production of certain types of radicals that lead to an improvement in the efficiency of the processes themselves. This gas has a significant impact on the environment because it causes the destruction of the ozone layer when it is found in the upper layers of the atmosphere, and after carbon dioxide and methane, it is the third gas in terms of its influence on global warming as well as on the absorption of infrared radiation in the atmosphere [3, 4]. It has been proposed as a potential replacement for gases with a much higher GWP (Global Warming Potential) such as SF_6 which is still used in the electronics industry as a gas insulator. Although the concentration of N_2O in the atmosphere is much lower than that of carbon dioxide and methane, there are numerous attempts to decompose this gas, together with other nitrogen oxides (NOx), by electrical discharges, that would lead to reduction of the damage and pollution they cause [5, 6, 7].

Despite of the great importance of this gas, the lack of reliable and complete cross section sets and transport and rate coefficients is evident, even in the case of a constant electric field, while there is no

data on the kinetics of electrons in the presence of a magnetic field. These data represent a critical point for modeling processes that lead to a further optimization of the application of the low temperature RF plasmas. Given the lack of the available transport data in RF fields, as well as the difficulty of including these coefficients in fluid and hybrid models due to their complexity, the only option for RF plasma modeling was the extrapolation of the available data for DC electric fields. The so-called quasi-static approximation was used at low field frequencies, while the effective field approximation was used in the case of high frequencies. Still, both approximations in the frequency range related to practical application are not very accurate. Likewise, in most of the earlier works related to plasma modeling, the effect of the magnetic field was not fully taken into account, which is in contrast to modern attempts at rigorous plasma models where the magnetic field sometimes plays a very important role.

Bearing in mind the large range of applications of this gas and the need for data on the kinetics of electrons under the influence of the magnetic field, starting from our previous study [12], we expanded out research to include these cases with an aim of checking which kinetic phenomena occurred during electron transport in N_2O and how they were related to the cross sections.

Monte Carlo (MC) code [8 – 11] was used to calculate the transport and rate coefficients of an electron swarm moving in N_2O gas under the influence of DC crossed electric and magnetic fields (mean energy, drift velocity, diffusion coefficients, rate coefficients for elastic and individual inelastic processes). Electron swarm of mean energy 1eV is released from the origin of the system, which is oriented so that the electric field has the direction of the *x*-axis, the magnetic direction of the *z*-axis, while the crossed electric and magnetic field direction is on the *y*-axis. For the initial particles we assume Maxwell's velocity distribution. The initial number of electrons varied from $2 \cdot 10^5$ to $5 \cdot 10^5$, except in the case of *B/N* = 2000 Hx, where $1 \cdot 10^5$ initial electrons were taken due to the difficult relaxation of the swarm. Calculations were performed for five different values of the reduced magnetic field (*B/N* = 100 Hx, 200 Hx, 500 Hx, 1000 Hx and 2000 Hx, 1Hx = 10^{-27} Tm^3), whereby the value of the reduced electric field *E/N* ranged from 50 Td to 2000 Td for each of these values *B/N*.

2. MATERIAL AND METHODS

2.1. Theoretical description of electron movement in dc electric and magnetic fields

The motion of charged particles within the swarm in an external electromagnetic field, ignoring the microscopic field originating from the particles themselves, is described by the equation:

$$m\dot{\vec{v}} = q\vec{E}(\vec{r},t) + q\vec{v} \times \vec{B}(\vec{r},t), \qquad (1)$$

where *m* and *q* are the mass and charge of electrons, $\vec{E}(\vec{r},t)$ and $\vec{B}(\vec{r},t)$ are the external electric and magnetic fields. Using one of the numerical techniques, it is possible to solve this equation and obtain particle trajectories.

If we observe the motion of an electron swarm under the influence of a stationary homogeneous magnetic field, the equation (1) becomes:

$$m\dot{\vec{v}} = q\vec{v} \times \vec{B}. \qquad (2)$$

By scalar multiplication of the previous equation by the particle velocity vector, we get that:

$$\frac{d}{dt}\left(\frac{1}{2}mv^2\right) = 0, \qquad (3)$$

from which we conclude that stationary and homogeneous magnetic fields change neither the intensity of the particle's velocity nor the kinetic energy. Solving the equation (2) shows that the path of the particle is a coil, along which the particle rotates around the line of force of the magnetic field with a frequency $\Omega = \frac{qB}{2\pi m}$, which is called a cyclotron frequency, and the movement of the particle itself is called cyclotron rotation. The pitch of the coil remains constant while its radius is given by the expression $r_L = \frac{v_\perp m}{qB}$, the so-called Larmor radius, which in this case remains constant ($v_\perp$ is the component of the particle velocity normal to the direction of the magnetic field). If the magnetic field is inhomogeneous, the path along which the particles move is no longer a coil of a constant pitch and radius, nor do the particles rotate around only one magnetic line of force.

The movement of a swarm of electrons under the influence of an electric field is described by the so-called total collision frequency v which contains frequencies for all possible collision processes among electrons and atoms (or molecules) of the target gas. As the number of collisions depends on

the energy of the electrons, their movement is determined by these collisions, i.e. by the strength of the external electric field that gives them energy and accelerates them along the mean free path. If the frequency ratio is $\frac{\Omega}{\nu} \ll 1$, the mode of movement of charged particles is collision dominated and in that case electrons do not manage to complete their circular paths due to frequent collisions with gas constituents, while for $\frac{\Omega}{\nu} \gg 1$ their motion is determined by the strength of the external magnetic field thanks to which electrons, in the time between collisions, manage to fully complete the individual cycles of their cyclotronic motion.

The Monte Carlo (MC) simulation code described in detail earlier [8-10] was used to calculate the transport coefficients. In the MC simulation, the motion of a large number of charged particles (in our case, electrons) is followed through a neutral background gas. A swarm of electrons of arbitrary initial energy is released from a coordinate origin with a Maxwell velocity distribution. The swarm moves under the influence of electric and magnetic fields, collides with gas or gas mixture constituents, and loses part of its energy while gaining more energy from the electric field. Electron scattering is considered isotropic and described by scattering cross sections, that are part of the input data. In addition to the cross section, the input data also include the gas concentration, which in all calculations was taken to be $3{,}54 \cdot 10^{22}$ m^{-3} corresponding to the pressure of 1 Torr (1 Torr = 133,322 Pa) at 273 K, molar mass of the main gas, the values of the reduced electric and magnetic fields (*E/N*, *B/N*) as well as the phase difference between them. It was assumed that the phase difference between the fields is 90°. In all simulations, the initial electron mean energy was assumed to be 1 eV, while the initial number of electrons varied from $2{,}5 \cdot 10^5$ to $5 \cdot 10^5$. The mean energy of the swarm, the drift velocity in the electric field direction ($W_{\vec{E}}$), the drift velocity in the direction normal to the plane in which the electric and magnetic fields are located ($W_{\vec{E}\times\vec{B}}$) and the total drift velocity ($W = \sqrt{W_{\vec{E}}^2 + W_{\vec{E}\times\vec{B}}^2}$) were calculated. Also, under the same conditions, diffusion coefficients in $\vec{E}$, $\vec{B}$ and $\vec{E} \times \vec{B}$ directions were determined. In some aspects of plasma modeling, it is necessary to know the rate coefficients for individual inelastic processes and those were calculated for several values of *B/N*.

The set of cross sections for the e^-/N_2O interaction used in the calculations as an input parameter is shown in Figure 1 and was obtained by the swarm method in our previous publication [12]. There are eleven individual processes, one elastic (line 2 in the Figure 1) and ten individual inelastic e^-/N_2O scattering processes (lines 3-13 in the Figure 1).

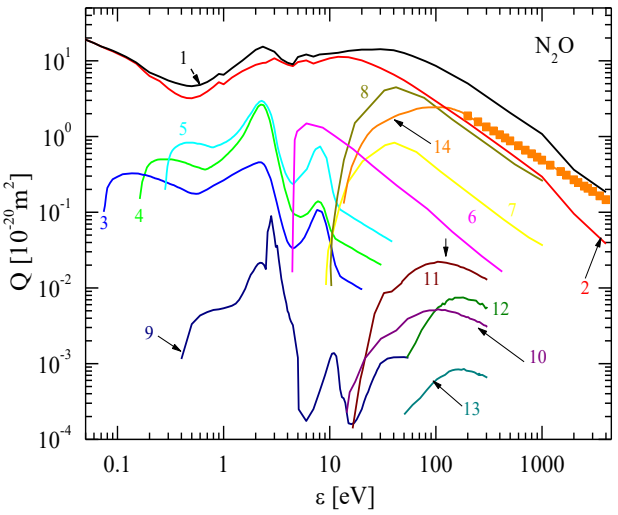

Figure 1. *The set of cross sections for e^-/N_2O interactions obtained by swarm technique: 1 – total; 2 – elastic; 3, 4 and 5 – vibrational excitations; 6, 7 and 8 – electronic excitations; 9 – dissociative attachment; 10, 11, 12 and 13 – dissociative electronic excitations; 14 – ionization, [12]*

3. RESULTS

3.1. Cyclotron and total collision frequency

Figure 2 (a) shows the cyclotron frequency (Ω) as a function of *E/N* for five values of *B/N* as may be trivially expected it depends only on the strength of the external magnetic field and increases with increasing *B/N*.

Figure 2 (b) shows the total collision frequency (*ν*), which represents the sum of the collision frequencies of all processes (elastic and inelastic). The first thing that is noticeable is that low values of *B/N* (100 Hx and 200 Hx) have almost no effect on *ν*, while with increasing *B/N*, *ν* starts to decrease. By increasing the *B/N*, the electron swarm deviates more and more from the direction of the external electric field, which reduces the possibility of gaining energy. In other words, the mean energy of the swarm decreases along with the total collision frequency. On the other hand, *ν* can also be related to the rate coefficients for elastic processes because they give

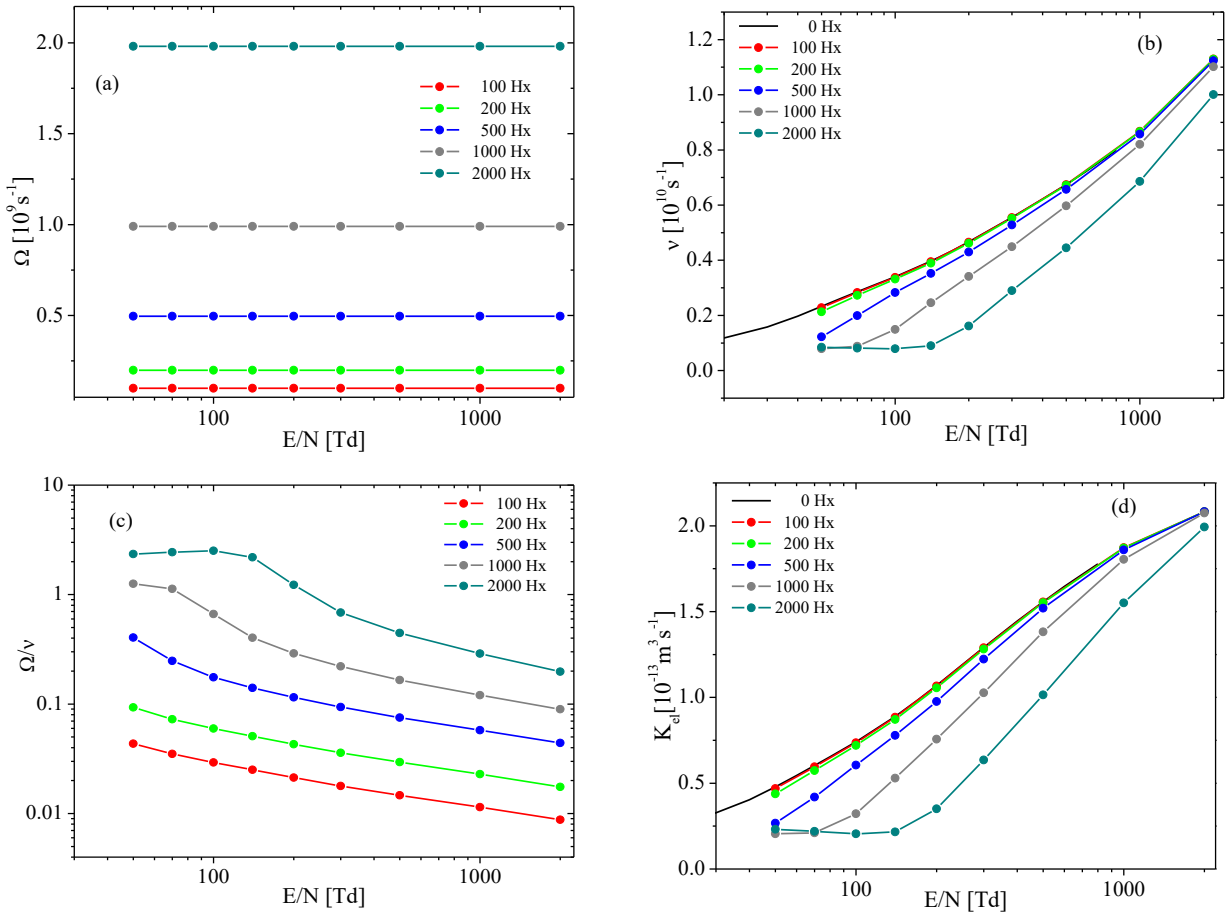

Figure 2. *(a) Cyclotron frequency, (b) Total collision frequency, (c) Ratio of cyclotron and total collision frequency, (d) Rate coefficient for elastic collision processes as a function of the reduced electric field for several different values of the reduced magnetic field*

the greatest contribution to the total collision frequency. Comparing the values of ν shown in Figure 2 (b) for different values of B/N and the values of rate coefficients for elastic processes shown in Figure 2 (d) for the same values of B/N (at the same points of E/N) shows that ν follows the behavior of these coefficients.

Figure 2 (c) displays the comparisons between the cyclotron and total collision frequencies. We see that this ratio is less than one for all B/N values, except in the case of the highest value of 2000 Hx (and for the smallest considered E/N values that are not sufficient for the swarm energy increase) when it is slightly above one. Consequently, we may suggest that in most of the considered cases swarm is in a collision-dominated mode, where electron transport is determined by the external electric field.

Rate coefficients for elastic collision processes (K_{el}) as a function of the reduced electric field for several different values of the reduced magnetic field are shown in Figure 2 (d). It is obvious that elastic rate coefficients for all values of B/N display similar behavior as total collision frequencies.

3.2. Mean energy

Figure 3 shows the mean energy of the electron swarm as a function of E/N, for several different values of B/N. We see that the cooling of the swarm, i.e. the reduction of its mean energy, occurs at higher values of B/N (higher than 200 Hx) and the reduction is greater at lower values of E/N. As E/N increases, the decrease in mean energy with increasing B/N is smaller because the strong electric field gives enough energy to the swarm before the strong magnetic field deflects it from its direction of motion. We see that the mean energy remains almost unchanged at 100 Hx and 200 Hx.

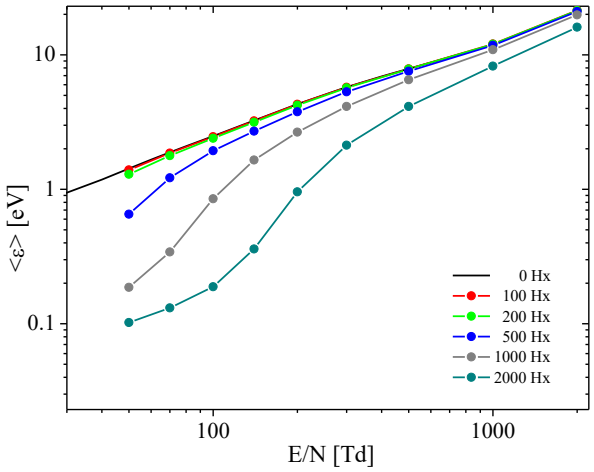

Figure 3. *Mean energy of the electron swarms as a function of E/N for five values of B/N, as well as in the case of B/N = 0 Hx.*

3.3. Drift velocity

During the transport of electron swarm in external crossed electric and magnetic fields, there are two drift velocity components: one in the electric field directions ($W_{\vec{E}}$) or longitudinal, and the other in the direction normal to the plane in which the electric and magnetic fields are located ($W_{\vec{E}\times\vec{B}}$), the so-called perpendicular component.

Figure 4 (a) shows the longitudinal component of the drift velocity as a function of *E/N* for some different values of *B/N*. We can see that at 100 Hx and 200 Hx this component has almost the same values (for the same *E/N*) as for *B/N* = 0 Hx. By further increasing the strength of the magnetic field, more and more electrons deviate from the direction of the electric field, which results in a decrease in the mean energy of the swarm, and thus a decrease in the drift velocity component in that direction. The longitudinal component increases with an increase of *E/N* for all values of *B/N* and does not show the energy structure of the cross section.

Figure 4 (b) demonstrates the drift velocity in the direction normal to the electric and magnetic field vectors $W_{\vec{E}\times\vec{B}}$. Contrary to the component $W_{\vec{E}}$, here we can see that with an increase of the magnetic field (for 100 Hx, 200 Hx and 500 Hx), for the same value of *E/N*, this component increases. For *B/N* = 1000 Hx, the values of the drift velocity at points up to 100 Td are smaller than those obtained for 500 Hx, while for *E/N* higher than 100 Td it increases again. This effect is even more pronounced at the highest value of *B/N* = 2000 Hx where the breaking point is shifted to *E/N* = 500 Td.

Figure 4 (c) shows the total drift velocity (*W*), i.e. the resultant of longitudinal and perpendicular components. We can see that *W* behaves similarly to the velocity component in the direction of the electric field, except that the decrease with increasing *B/N* is smaller due to the influence of the perpendicular component.

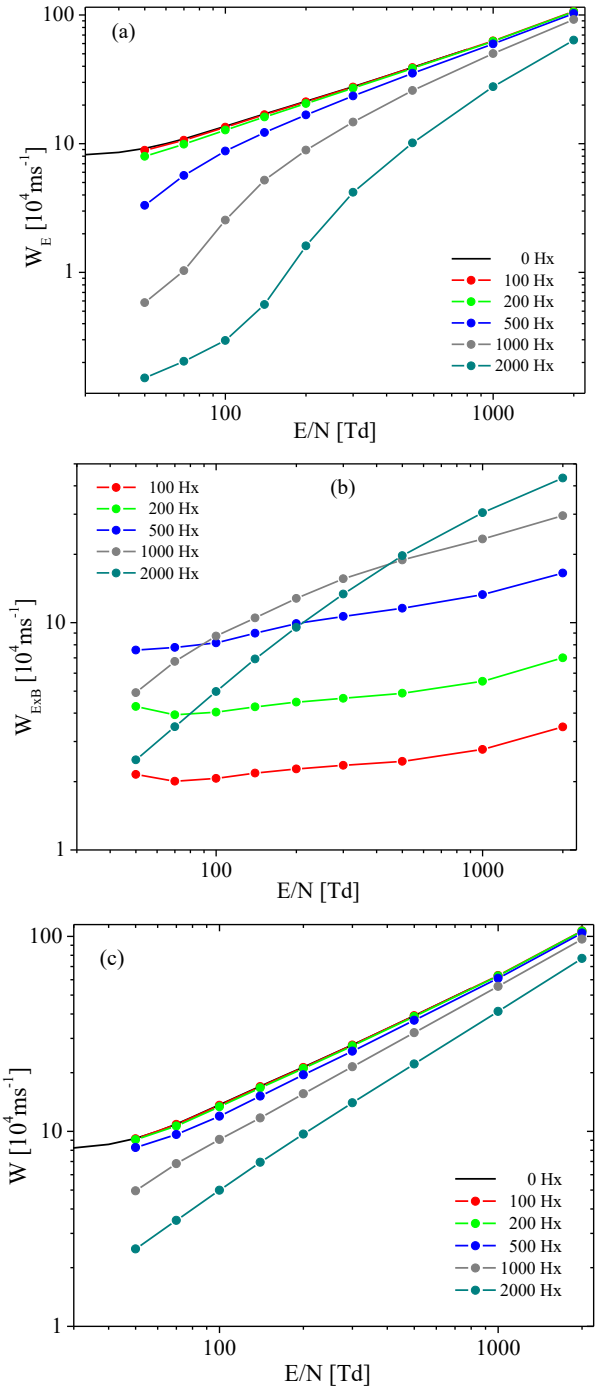

Figure 4. *Electron drift velocity: (a) longitudinal component of the drift velocity, (b) perpendicular component of the drift velocity, (c) total drift velocity*

3.4. Diffusion coefficients

Figure 5 (a) shows the diffusion coefficient in the direction of the electric field ($ND_{\vec{E}}$) as a function of *E/N* for five values of *B/N*, as well as the absence of a magnetic field when the coefficients in both directions ($\vec{B}$ and $\vec{E} \times \vec{B}$) are equal and represent the transverse diffusion coefficient. We can see that low values of *B/N* (100 Hx and 200 Hx) do not affect the diffusion in $\vec{E}$ direction that starts to decrease only at *B/N* = 500 Hx, and then even more as *B/N* increases further. If we look at the dependence of this coefficient on the electric field, we see that for the two highest considered values of *B/N* (1000 Hx and 2000 Hx) the diffusion coefficient in $\vec{E}$ direction increases very quickly with an increase of *E/N* (up to 200 Td) and then enters the area of a slightly slower growth. From the cross sections set for the e^-/N_2O interaction (Figure 1), we see that the area of rapid growth of the diffusion coefficient in $\vec{E}$ directions corresponds to the area of medium electron energies for which vibrational processes and electron attachment decrease rapidly, which facilitates diffusion. With the increase in *E/N*, we enter the area of medium energies in which new inelastic processes of electronic excitations and ionization occur at higher energies and hinder diffusion so a slightly slower growth of the diffusion coefficient follows.

The diffusion coefficient in the direction of the magnetic field ($ND_{\vec{B}}$) shown in Figure 5 (b) behaves in a similar way, as well as in the direction normal to the direction of the electric and magnetic fields ($ND_{\vec{E}\times\vec{B}}$), as shown in Figure 5 (c).

Figure 5 (d) shows the ratio of diffusion coefficients in the direction of the electric and magnetic fields. We can see that this ratio is close to unity at

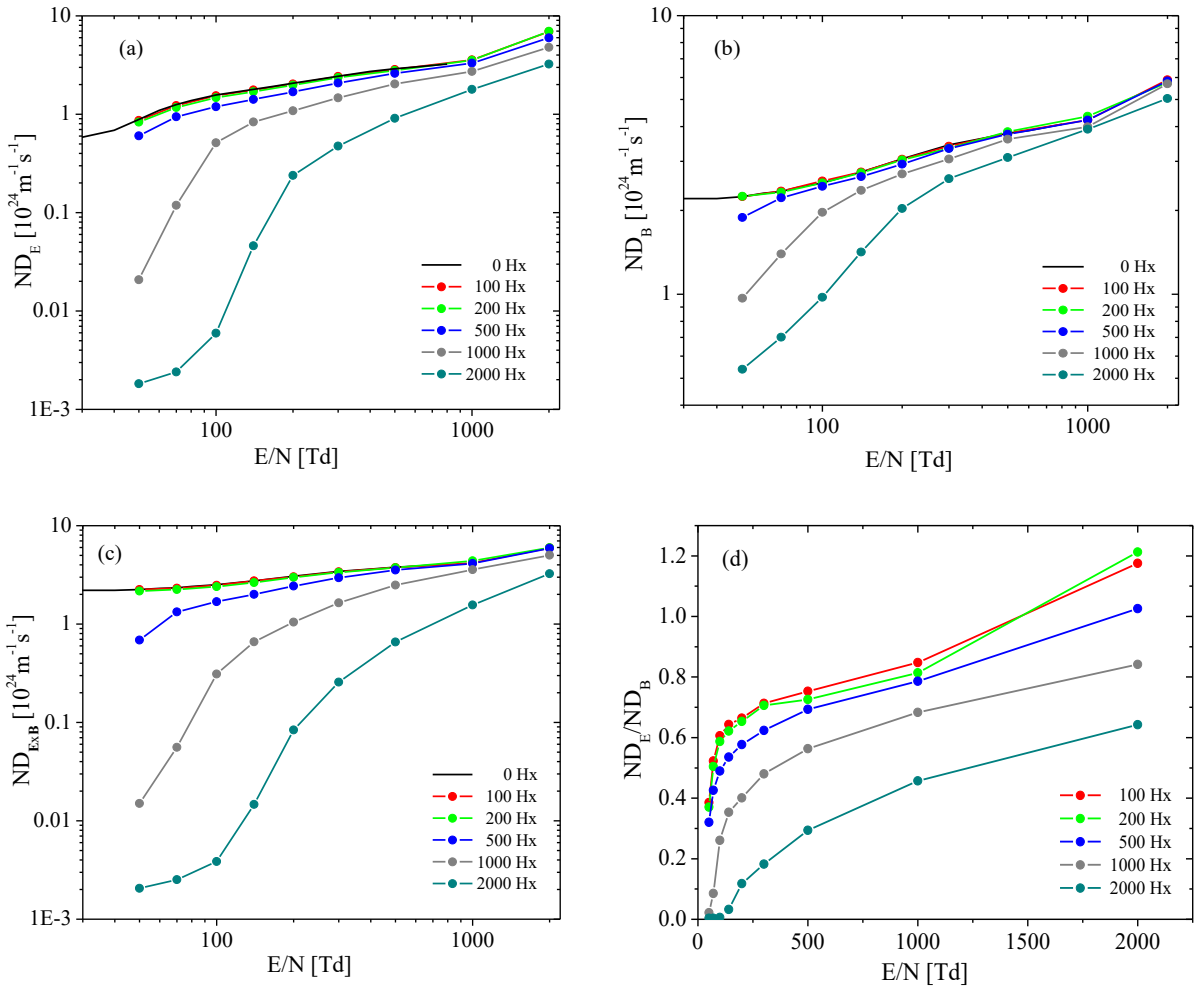

Figure 5. *Diffusion coefficients as a function of E/N for five values of B/N: (a) in the direction of the electric field, (b) in the direction of the magnetic field, (c) in the direction normal to the direction of the electric and magnetic fields, (d) The ratio of diffusion coefficients in the direction of the electric and magnetic fields.*

lower *B/N* values (100 Hx and 200 Hx) and higher *E/N* values (500 Td and higher), while as B/N increases, their ratio decreases. We can conclude that electron diffusion in N_2O is slightly anisotropic and that the anisotropy is more pronounced with the higher intensity of the reduced magnetic field.

3.5. Rate coefficients for inelastic processes

Figure 6 (a, b and c) shows the rate coefficients for vibrational excitation processes (cross sections 3, 4 and 5 in Figure 1) as a function of *E/N* for different values of *B/N*. All three coefficients (K_{v1}, K_{v2}, K_{v3}) behave in a similar fashion.

At low B/N all three curves are similar in shape showing negligible effect of magnetic field (point of maximum) although the curves differ considerably in the magnitude. As Magnetic field rises beyond 200 Hx the effect of magnetic field depletes rates at lower E/N and the maximum of the rate start moving towards higher E/N.

Figure 7 (a, b and c) shows the rate coefficients for electronic excitation processes (cross sections 6, 7 and 8 in Figure 1). As we can see in the figure, all three coefficients (K_{exc1}, K_{exc2} and K_{exc3}) at lower *E/N* decrease with an increase in *B/N*. At higher *E/N*, the reduction of these coefficients is less pronounced, while at the highest values the magnetic field has almost no effect.

Figure 8 (a) shows the rate coefficient for the dissociative electron attachment process $K_{d.att}$. Cross section for the electron attachment to the molecule N_2O is shown in Figure 1 for process number 9. If we observe the influence of the magnetic field

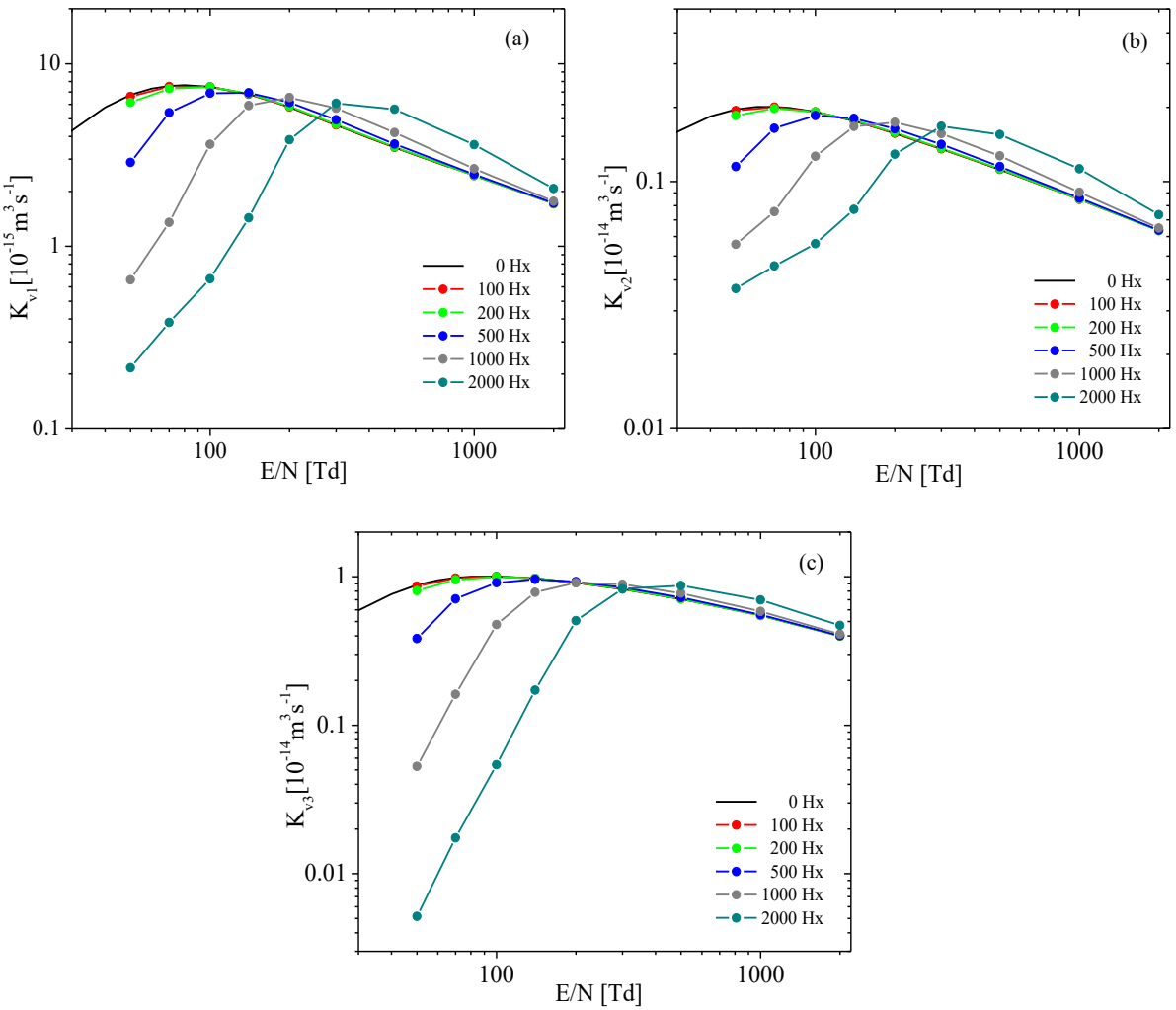

Figure 6. *Rate coefficients for vibration processes shown in Figure 1 with lines 3, 4 and 5; (a) K_{v1} with energy threshold $\varepsilon_{th} = 0.1593$ eV , (b) K_{v2} with energy threshold $\varepsilon_{th} = 0.073$ eV , (c) K_{v3} with energy threshold $\varepsilon_{th} = 0.2757$ eV, as a function of E/N for different values of B/N.*

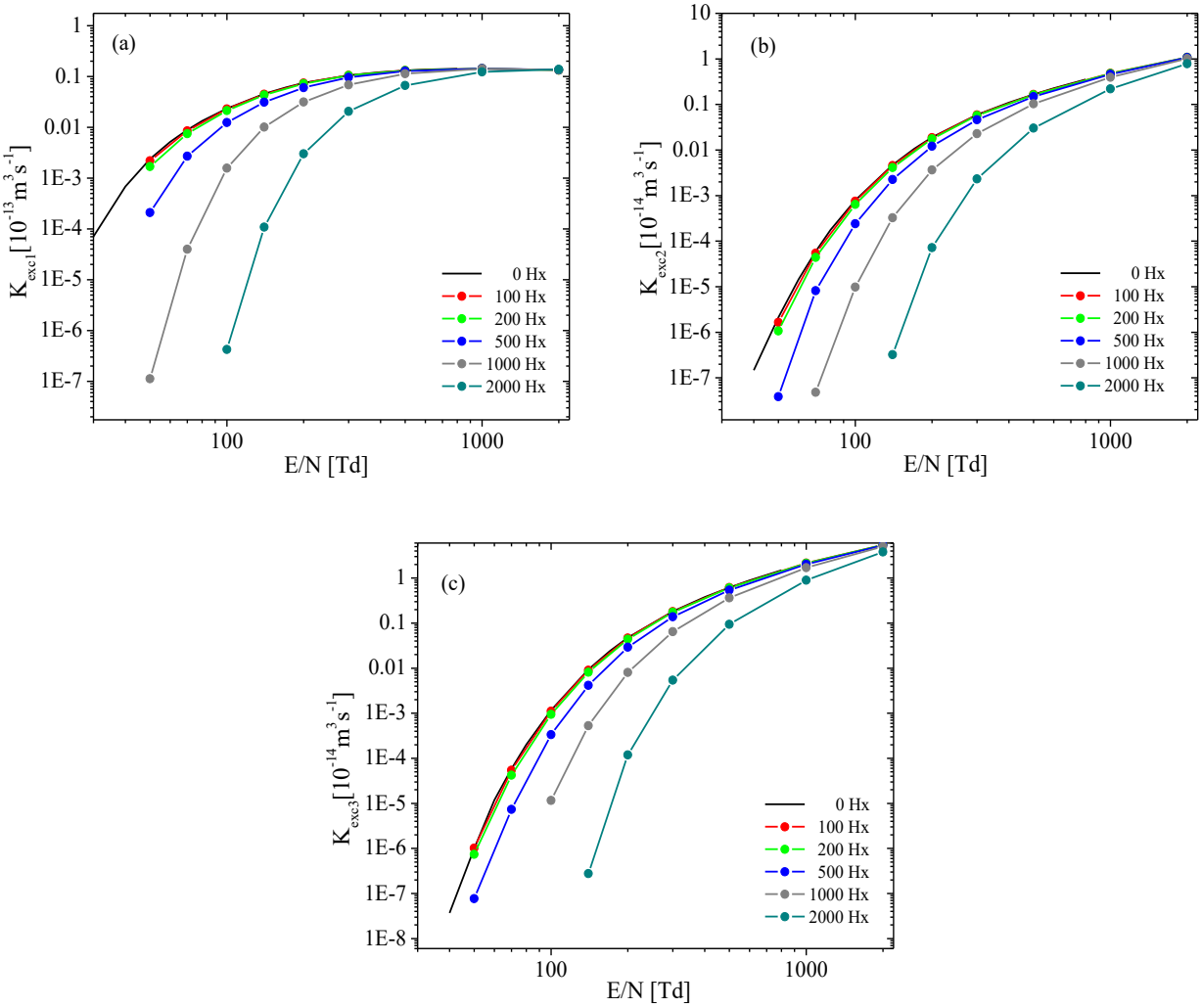

Figure 7. *Rate coefficients for excitation processes shown in Figure 1 with lines 6, 7 and 8; (a) K_{exc1} with energy threshold $\varepsilon_{th} = 4.0$ eV, (b) K_{exc2} with energy threshold $\varepsilon_{th} = 8.5$ eV, (c) K_{exc3} with energy threshold $\varepsilon_{th} = 9.6$ eV, as a function of E/N for different values of B/N.*

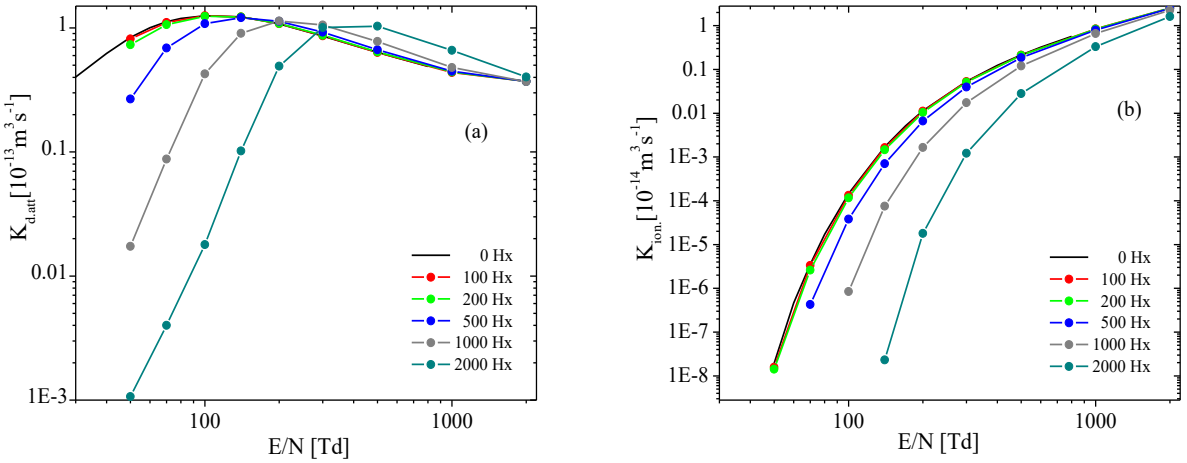

Figure 8. *Rate coefficients for the processes of (a) dissociative attachment and (b) ionization, as a function of E/N for five values of B/N.*

on this coefficient, we see that there are two areas, the area of low values of *E/N* (up to 140 Td) in which the values of this coefficient (for the same E/N) decrease by orders of magnitude as *B/N* increases, and the area of higher values of *E/N* (greater than 140 Td) in which its values increase (for the same E/N) as *B/N* increases. In the first area, the electric field is not strong enough to compensate for the loss of energy due to the increase in the magnetic field, while in the second area, despite the strong magnetic field that cooled the electron swarm, the electric field is strong enough to compensate for this loss. If we observe this coefficient for the same value of *B/N*, we see that in all five cases of *B/N* it increases with an increase of *E/N* to a maximum and then decreases as *E/N* increases further.

Figure 8 (b) displays the rate coefficient for the ionization process as a function of *E/N*. We see that the values of this coefficient decrease (for the same *E/N*) as *B/N* increases and that the shape of the rate coefficient function corresponds to the energy dependence of the ionization cross section (Figure 1, line 14).

4. CONCLUSION

The paper presents and discusses the results obtained by considering electron transport in nitrous oxide (N_2O) under the influence of DC crossed electric and magnetic orthogonal configuration fields. Our MC simulation code was used for calculations of transport and rate coefficients. Calculations were made for several values of the reduced magnetic field (*B/N* = 100 Hx, 200 Hx, 500 Hx, 1000 Hx and 2000 Hx, 1Hx = 10^{-27} Tm^3), where the amplitude of the reduced electric field varied for each *B/N* field in the interval from 50 Td to 2000 Td (1Td = 10^{-21} Vm^2). Our set of the cross sections for e^-/N_2O scattering was used as an input in the simulations.

The results obtained by MC simulations [13 - 15] are shown in Figures 1 – 8 and can be used as input data for plasma modeling for this gas. The cyclotron and total collision frequency, mean swarm energy, electron drift velocity, both total and in the $\vec{E}$ and $\vec{E} \times \vec{B}$ directions, diffusion coefficients and rate coefficients for elastic and individual inelastic processes were calculated.

The ratio of cyclotron to total collision frequency in this specific case is less than one (except for the highest value when it is slightly greater than one) for all values of *B/N* so we may suggest that our swarm is in a collision-dominated mode. The cooling effect of the swarm is evident, as well as a decrease in the drift velocity component in the direction of the electric field. Diffusion is slightly anisotropic because the ratio of diffusion coefficients in the $\vec{E}$ and $\vec{B}$ directions is close to unity. Getting acquainted with the so-called kinetic phenomena in gas discharges as covered by this work is essential for potential applications of such plasmas. [14,16].

5. REFERENCES

[1] H. Matsui, et al., *N doping using N_2O sources: From the viewpoint of ZnO*, J. Appl. Phys., 95, (2004), 5882–5888.

[2] Y. Kim, et al., *Plasma reactions of N_2O on hydrogenated amorphous carbon films by PECVD*, Surface and Coatings Tech., 180–181, (2004), 250–253.

[3] P. J. Crutzen, *Ozone production rates in an oxygen-hydrogen-nitrogen oxide atmosphere*, Journal of Geophysics Research, 76, (1971), 7311–7327.

[4] T. E. Graedel and P. J. Crutzen, *Atmospheric Change: An Earth System Prospective,* Freeman, New York, (1993).

[5] A. Mizuno et. al., *NOx removal process using pulsed discharge plasma*, IEEE Trans. Ind. Applicat., 31, (1995), 957–964.

[6] S. Masuda and H. Nakao, *Control of NOx by positive and negative pulsed corona discharges*, IEEE Trans. Indus. Appl., 26, (1990), 374–383.

[7] Y. S. Mok et. al., *Abatement of Nitrogen Oxides in a Catalytic Reactor Enhanced by Nonthermal Plasma Discharge*, IEEE Trans. Plasma Sci., 31, (2003.), 157–165.

[8] K. Maeda et al., *Diffusion tensor in Electron Transport in gases in a radiofrequency Field*, Phys. Rev. E, 55, (1997), 5901.

[9] Z. R. Raspopović et. al., *Benchmark Calculations for Monte Carlo Simulations of Electron Transport*, IEEE Trans. Plasma Sci., 27, (1999), 1241–1248.

[10] Z. Ristivojević and Z. Lj. Petrović, *A Monte Carlo simulation of ion transport at finite temperatures*, Plasma Sources Sci. Technol., 21, (2012), 035001.

[11] S. Dujko, *The multi-term Boltzmann equation analysis and Monte Carlo study of hydrodynamic and non-hydrodynamic charged particle swarms*, PhD Thesis, James Cook University, (2009).

[12] S. Dupljanin et al., *Transport coefficients and cross sections for electrons in N_2O and N_2O/N_2 mixtures*, Plasma Sources Sci. Technol., 19, (2010), 025005.

[13] Z. Lj. Petrović et al., *Kinetic phenomena in electron transport in radio-frequency fields,* Applied surface science, 192, (2002), 1-25.

[14] Z. Lj. Petrović et al. *Measurement and interpretation of swarm parameters and their application in plasma modelling*, J. Phys. D: Appl. Phys., 42, (2009), 194002.

[15] Z Raspopović et al. *Diffusion of electrons in time-dependent E (t)× B (t) fields*, Journal of Physics D: Applied Physics, 33, (2000), 1298.

[16] I. Adamovich et al., *The 2017 Plasma Roadmap: Low temperature plasma science and technology*, J. Phys. D: Appl. Phys., 50, (2017), 323001.

ТРАНСПОРТНЕ КАРАКТЕРИСТИКЕ ЕЛЕКТРОНА У АЗОТ-СУБОКСИДУ (N_2O) У УСЛОВИМА ДЈЕЛОВАЊА КОНСТАНТНИХ ОРТОГОНАЛНИХ ЕЛЕКТРИЧНИХ И МАГНЕТНИХ ПОЉА

Сажетак: У раду су приказани и дискутовани резултати Монте Карло (МС) прорачуна транспортних и брзинских коефицијената роја електрона који се крећу у азот-субоксиду (N_2O) под дејством константних укрштених електричних и магнетних поља ортогоналне конфигурације. Као улазни параметар коришћен је скуп ефективних пресјека за e^-/N_2O расејање добијен у нашим ранијим истраживањима. Прорачуни средње енергије, брзине дрифта, дифузионих коефицијената као и брзинских коефицијената за еластични и појединачне нееластичне процесе извршени су за неколико различитих вриједности редукованог магнетног поља (*B/N* = 100 Hx, 200 Hx, 500 Hx, 1000 Hx and 2000 Hx, 1Hx = 10^{-27} Tm^3). За сваку испитивану вриједност амплитуде *B/N* варирана је вриједност амплитуде редукованог електричног поља (*E/N*) у интервалу од 50 Td to 2000 Td (1Td = 10^{-21} Vm^2). Однос циклотронске и укупне колизионе фреквенције је за све испитиване вриједности *B/N* мањи од један, изузев највеће вриједности од 2000 Hx, када је тај однос незнатно већи од један, те можемо рећи да се ради о сударно доминантном режиму. Видљив је ефекат хлађења роја који се огледа у смањењу његове средње енергије порастом амплитуде *B/N* као и смањење компоненте брзине дрифта у правцу електричног поља. За највише вриједности *B/N* дифузија електрона је благо анизотропна.

Кључне ријечи: рој електрона, транспортни коефицијенти, азот-субоксид.

Paper received: 25 August 2023 **Paper accepted: 27 November 2023**